Influence of local surface texture by tool impression on the self-piercing riveting process and the static lap shear strength

Dezhi Li

WMG, University of Warwick, Coventry, CV4 7AL, UK

Tel: +44 (0)2476574614, Fax: +44 (0)2476575366, E-mail: dezhi.li@warwick.ac.uk

Abstract

To increase fuel efficiency and reduce emission, aluminium alloys have been increasingly used in automotive body-in-white structures for lightweighting. Due to its advantages over some of the more traditional joining technologies, self-piercing riveting (SPR) has been widely used for these lightweight structures. Research has showed that friction is a very important factor that influences both the riveting process and joint strength for SPR, but these influences have not been fully understood. In this paper, an innovative method was used to modify the local surface of the top sheet around the rivet piercing location with different impression tools (the central pin, the small ring, the medium ring and the large ring) and garnet particles to study the influence of local frictions on rivet inserting process, joint features and static lap shear strength. The results showed that the local surface textures on the aluminium sheet did not have significant influence on the rivet inserting process based on displacement-force curve analysis. The local surface textures could slightly change the joint features, especially the rivet head height, but overall this influence was not significant. The lap shear tests showed that ring impressions with garnet particles and central pin impressions on the bottom surface of the top sheet increased the static lap shear strength of the SPR joints. The results confirmed that the critical location for local friction influence on the lap shear strength was around the rivet leg piercing location.

Key Words: Self-piercing riveting; surface texture; tool impression; friction; lap shear strength

1. Introduction

In order to increase fuel efficiency and reduce CO_2 emission, aluminium is increasingly used in automotive body-in-white structures for lightweighting. Self-piercing riveting (SPR) is one of the main joining methods for aluminium and mixed material structures due to its advantages in clean working environment, ability to join dissimilar materials, low energy requirement and high static and fatigue joint strengths etc. [1].

Friction is an important factor for installation and strength of mechanical joints. For example, the friction between the bolt, nut and joint members will influence the tighten torque applied to the joint members of the bolted joints and the friction between the joint members will contribute or decide the shear strength of the bolted joints [2, 3]. As a mechanical joining process, friction is very important for both the SPR rivet setting process and joint strength due to the relative movements between different components, and the frictions existing in a SPR setting process or a SPR joints can be between sheet materials and between rivet and sheet materials. As we know, friction between two surfaces is related with the surface conditions. To find out the influence of surface conditions and friction on SPR setting process and joint strength, some research had been conducted [4-7] . These research on the influence of surface conditions on SPR joint quality and performance have been reviewed by Li et al [1].

Han and Chrysanthou [4] and Han et al. [7] studied the influence of coatings on sheet material on the joint quality and mechanical strength of SPR joints. In their study, AA5754 was used as the top sheet, and HSLA 350 with different coatings, i.e. uncoated, e-coated and zinc plated, was used as bottom sheet. Their results showed that the extent of the effects of surface coatings on the joint quality and mechanical behaviour of SPR joints differed significantly with different types of coatings on the HSLA steel. Han et al. [5] studied the influence of sheet/sheet interfacial condition on the fatigue performance of SPR joints. The results showed that the presence of a wax-based solid surface lubricant could delay the onset of fretting damage on the alloy surface, leading to extended fatigue life; the application of a PTFE insert at the interface between the riveted sheets eliminated or significantly reduced fretting damage, but led to a reduction in the fatigue life due to a different failure mode. Research from Li et al. [6] showed that fretting during fatigue increased the surface roughness, which consequently increased the remaining static lap shear strength of the specimens due to the increased friction force between the tip of the punched hole in the top sheet and the edge of the partially pierced hole in the bottom sheet.

Friction is also a very important aspect for SPR simulation. In the models for simulation, different researchers have used different coefficients of friction. A value of 0.1 was used by Xu [8], a value of 0.15 was used by Khezri et al. [9], and a value of 0.2 was used by Abe et al. [10], for all interfaces. Other researchers used different friction coefficients at different locations. For example, Krishnappa [11] used the friction coefficients of 0.15 and 0.3 at different locations. Atzeni et al. [12] used a friction coefficient of 0.2 for the interfaces between the punch and the rivet and between the rivet and the sheet, a friction coefficient of 0.1 for the interface between the bottom sheet and the die, and a friction coefficient of 0.15 for the interface between the top and bottom sheets. In the model used by Carandente et al. [13], the friction coefficient used for the interface between the top and bottom sheets, the interface between the bottom sheet and the die, and the interface between the top sheet and the blank holder were 0.09, 0.15, and 0.15, respectively. However, to find out the actual friction coefficients at different interfaces is quite difficult due to the variation of applied pressure and surface texture etc.

Apart from conventional SPR, the influence of friction on flat-bottom self-piercing riveting (different from convenient SPR, a flat plate is used instead of a die with a cavity) was also studied. Han et al. [14] studied the influence of friction on the joint quality of flat-bottom self-piercing riveted AZ31 magnesium alloy joints through simulation. The friction at different locations, between the bank holder and the top sheet, between the rivet and the sheet materials, between the top and the bottom materials and between the bottom sheet material and the bottom plate, was studied, and the recommended friction coefficients at the above-mentioned locations were 0.2, 0.1, 0.5 and 0.4, respectively.

The friction during a SPR rivet setting process and in a joint load sustaining state is very complex due to the existing of multiple friction interfaces. Currently, no critical friction locations have been confirmed through experiments or simulation, and the influence mechanisms of friction on rivet setting and joint strength need further understanding. In order to find out some of the critical friction locations for SPR, in this paper, the influence of local surface textures of aluminium AA5754 by tool impression on rivet inserting process, joint features and static lap shear strength was studied.

2. Experimental procedure

2.1. Materials

The material used in this study is 2.0 mm thick AA5754 with a standard PT2 pretreatment and an AL070 wax lubricant. The AA5754 has an UTS, a yield strength and an elongation of 241 MPa, 110 MPa and 25%, respectively.

2.2. Local surface modification

In order to see the influence of local surface texture, especially roughness, on the SPR riveting process and joint strength, the bottom surface of the top sheet before rivet inserting was modified using various impression tools listed in Fig. 1, at the locations indicated in Fig. 2. The impression tools were custom made so that it can be attached to the nosepiece of our Henrob SPR gun, as shown in Fig. 3. A pre-set force from the SPR gun used for stack thickness measurement, 8kN, was used for the impression. A dummy die (top face diameter, 18 mm) without any cavity was used to support the sheet material. For joint quality analysis and SPR setting process study, 38 mm square coupons were used, and for lap shear specimens, 111.5 mm x 48 mm coupons were used. For one surface modification, the impression was conducted on the top surface of the top sheet with the central pin to see the influence of local deformation on joint features and lap shear strength. All other impressions were done with the top sheet upside down, and custom made fixtures were used to insure that when the coupon was turned over, the impression would still be at the same location. Since the impressions may introduce work hardening in addition to surface texture, it is essential to separate the influence of work hardening from the influence of surface texture. It is assumed that the impressions with tools without particles would only introduce work hardening, because it did not make the surface rougher. For this reason, some of the impressions were done with the impression tools only to see the influence of potential work hardening. Most of the impressions were done with the impression tools and small garnet particles for grit blasting. Among the coupons modified with the impression tools and garnet particles, half of them, particles were remained on the impression location, and the other half, particles were removed with fingernails as much as possible although some particle residuals must be still trapped in. Totally 15 stacks were evaluated, and the base stack is 2 mm AA5754 joined to 2 mm AA5754.

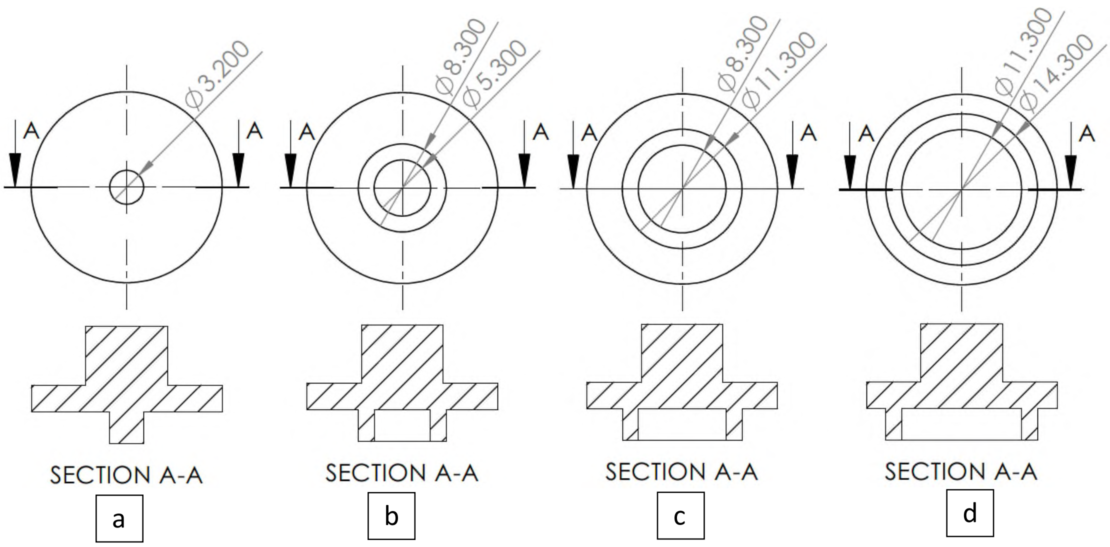

Figure 1 Geometries of the impression heads, a), with a central pin, b), with a small ring, c), with a medium ring and d) with a large ring (unit, mm).

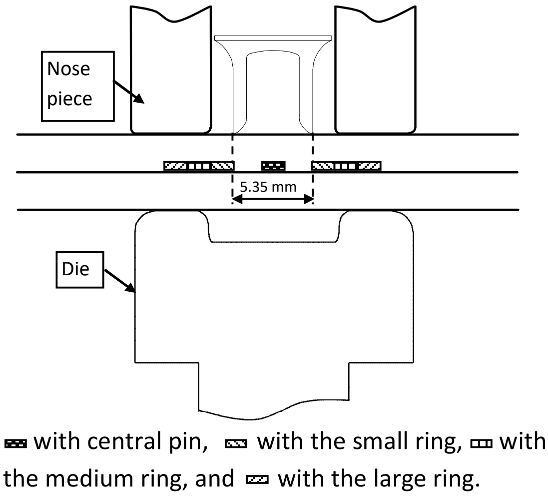

Figure 2 Locations of local impression and surface modification on the bottom surface of the top sheet before rivet inserting.

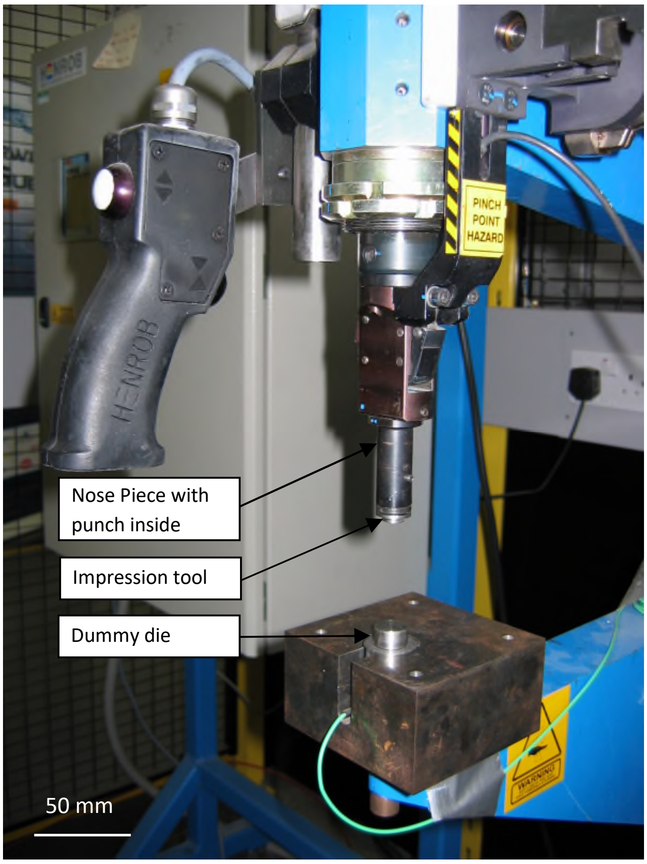

Figure 3 SPR gun with one impression tool and the dummy die.

2.3. Sample preparation

For all stacks, steel rivets from Henrob Ltd. with a countersunk head and mechanical zinc/tin surface coating were used. All specimens were joined with a Henrob servo-driven SPR system. A location fixture was used to make sure that in all samples the rivets will be set in the same locations. A rivet/die/velocity combination was used to achieve good joint quality, as listed in Table 1. The displacement-force curves for rivet inserting processes were recorded with an Emhart Tucker SPR system with the same rivet/die combination and an equivalent setting force. Joint quality of specimens was inspected through cross-sections. A special fixture was used to ensure all joints were vertically cross-sectioned through the centre of the rivets in transverse direction. The joint features, including rivet head height, interlock and minimum remaining bottom material thickness (T_{min}), from the cross-sections were measured and analyzed using the Aquinto a4i image analysis software. At least three joint coss-sections were measured for each joint combination.

Table 1 Optimum SPR parameters for (2+2)AA5754 stack-up.

Rivet	Length: 6.5 mm; Stem diameter: 5.35 mm; Type: countersunk; Hardness: ~410Hv
Die	Cavity diameter: 9 mm; Cavity depth: 2 mm; Type: flat bottom
Velocity	100 (Henrob unit, determining applied force)

Specimen geometries and dimensions for lap shear tests are shown in Fig. 4. All coupons were cut from sheet with the longitudinal direction of coupons (loading direction during subsequent mechanical tests) coincides with the rolling direction of sheet metal. To reduce any variations of rivet position, a custom designed fixture was used to set rivets into correct positions in Fig. 4. For each specimen, 48 mm wide coupons were used, and two rivets were set with an edge distance of 11.5 mm. The edge distance was recommended by Li et al. [15, 16] for optimized static and fatigue performance.

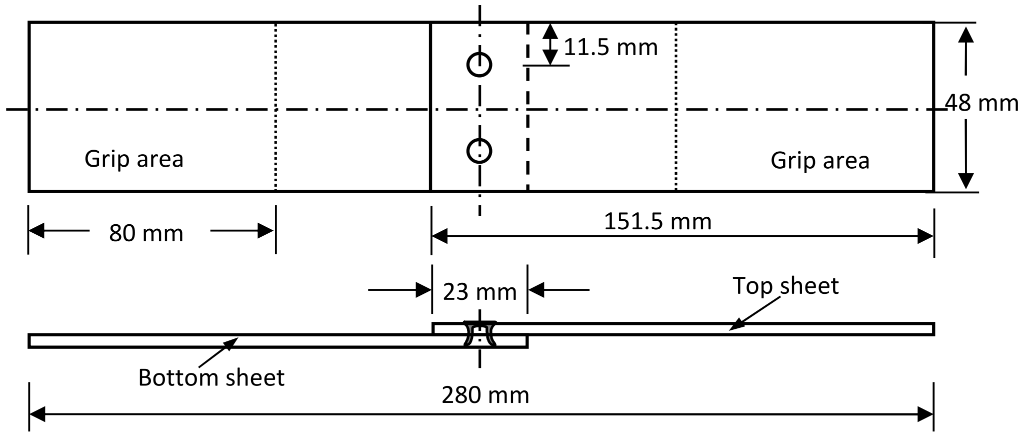

Fig. 4. Specimen geometry for lap shear tests.

2.4. Mechanical tests

Mechanical tests were conducted by following the company standards. An Instron with cross-head speed of 10 mm/min was used for the static tests, and 2 mm thick spacers were applied at both ends of the lap-shear samples to minimize coupon bending during lap-shear testing. At least three specimens were tested for each joint combination.

3. Results

3.1. SPR joint quality

Fig. 5 shows a cross section of the reference SPR joint studied in this paper. The SPR joint quality attributes have been annotated and these are rivet head height of -0.08 mm, an average interlock of 0.77 mm, and a minimum remaining bottom material thickness of 0.68 mm.

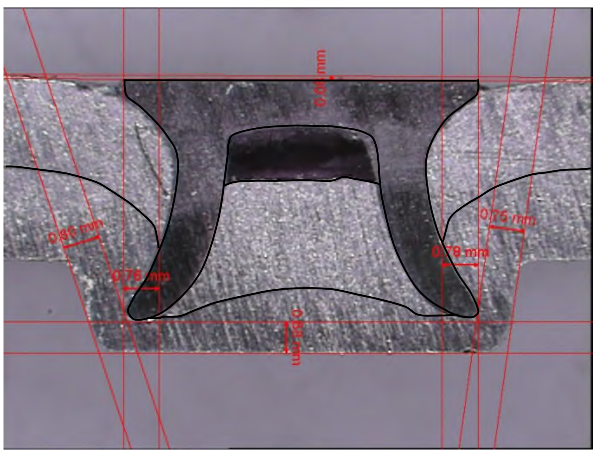

Figure 5 Cross section of a reference (2+2)AA5754 SPR joint with original surface texture and lubricant.

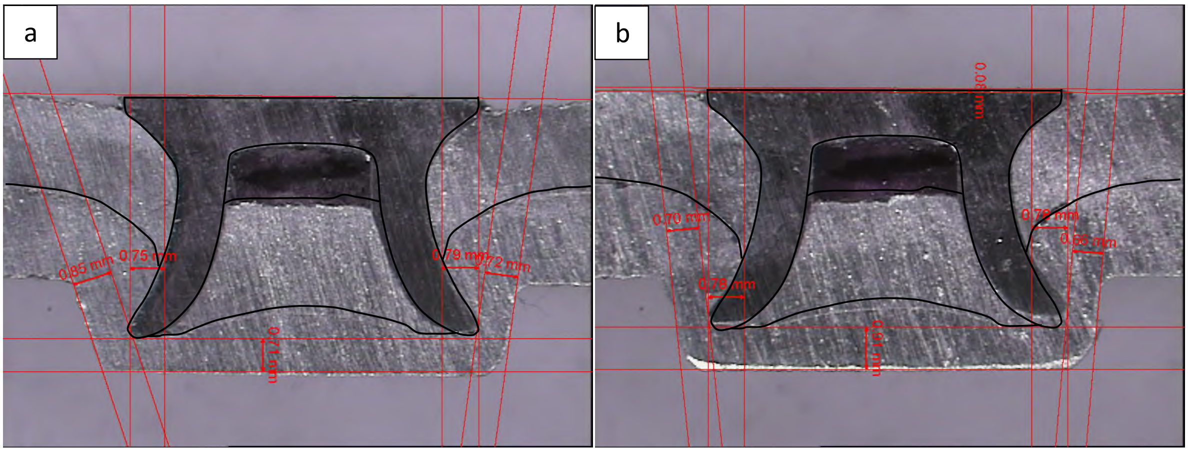

Figure 6 Cross section of (2+2)AA5754 SPR joints with the bottom surface of the top sheet impressed by a small ring and garnet particles, a) with particles removed, and b) with particles remained (the black outline is the profile of the deformed rivet and sheet materials in the reference joint).

Fig. 6 shows the cross sections of (2+2)AA5754 SPR joints with the bottom surface of the top sheet impressed by a small ring with garnet particles. By comparing the cross sections in Figs. 5 and 6, it can be seen that when the local areas were modified by the small ring with or without particles removed, the rivet head height was getting higher and the interlock and overall T_{min} were similar, although the T_{min} to the bottom of the joint button increased. It can be seen that due to increased friction at ring impression location, the plastic flow of the bottom sheet into the die cavity was getting more difficult. As a result, more resistance to rivet inserting would be from the bottom material between the rivet legs and the side of the die and less resistance would be from the material between the punched top sheet and the bottom of the die, although in this case the influence was not significant. It can also be seen that for joints with local areas modified by the impression ring, the cavity under the rivet head and above the punched top sheet became larger compared with the reference joints, which meant less force was used to push the punched top material into the rivet cavity.

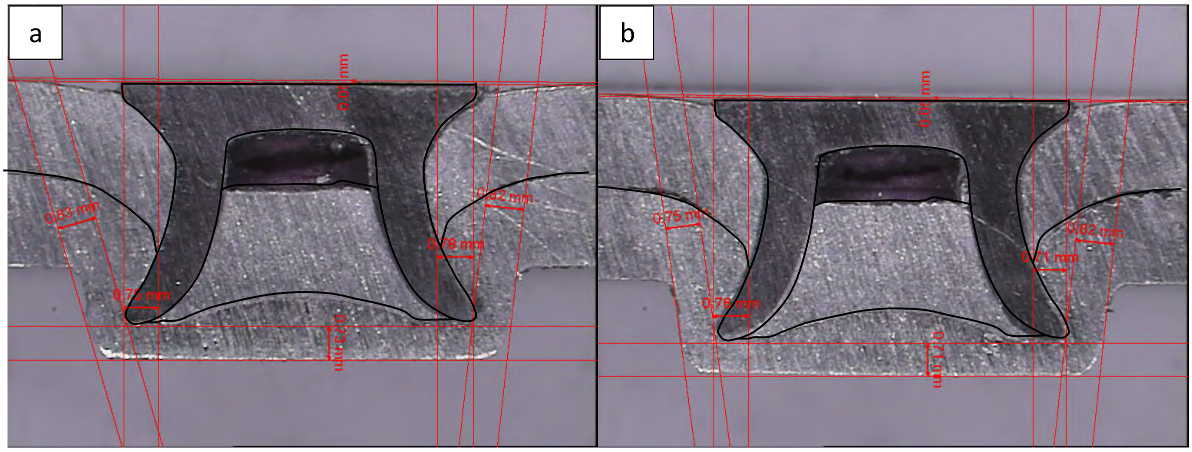

Figure 7 Cross section of (2+2)AA5754 SPR joints with the bottom surface of the top sheet impressed by a medium ring and garnet particles, a) with particles removed, and b) with particles remained.

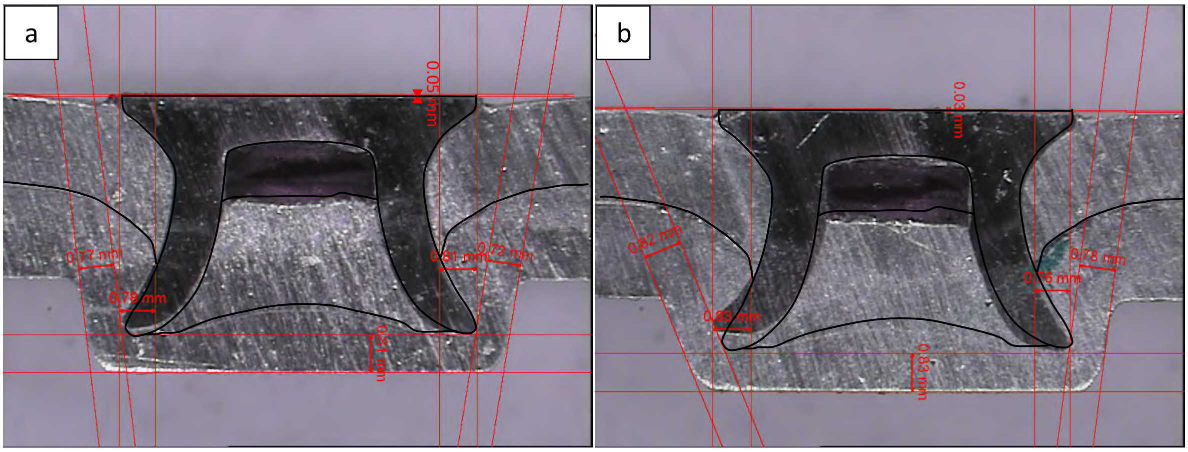

Figure 8 Cross section of (2+2)AA5754 SPR joints with the bottom surface of the top sheet impressed by both small and medium rings and garnet particles, a) with particles removed, and b) with particles remained.

Figs. 7 and 8 show the cross sections of (2+2)AA5754 SPR joints with the bottom surface of the top sheet impressed by a medium ring and a combination of small and medium rings with garnet particles, respectively. Similar influence on rivet setting as that for joints with the impression with the small ring could be seen. The deformation of rivet legs in Fig. 8b was unbalanced, which may be caused by the slight misalignment of the top and the bottom sheets after ring impression during rivet inserting. From Figs 6-8, it can be seen that the influence of local surface modification from the medium ring was smaller than that from the small ring.

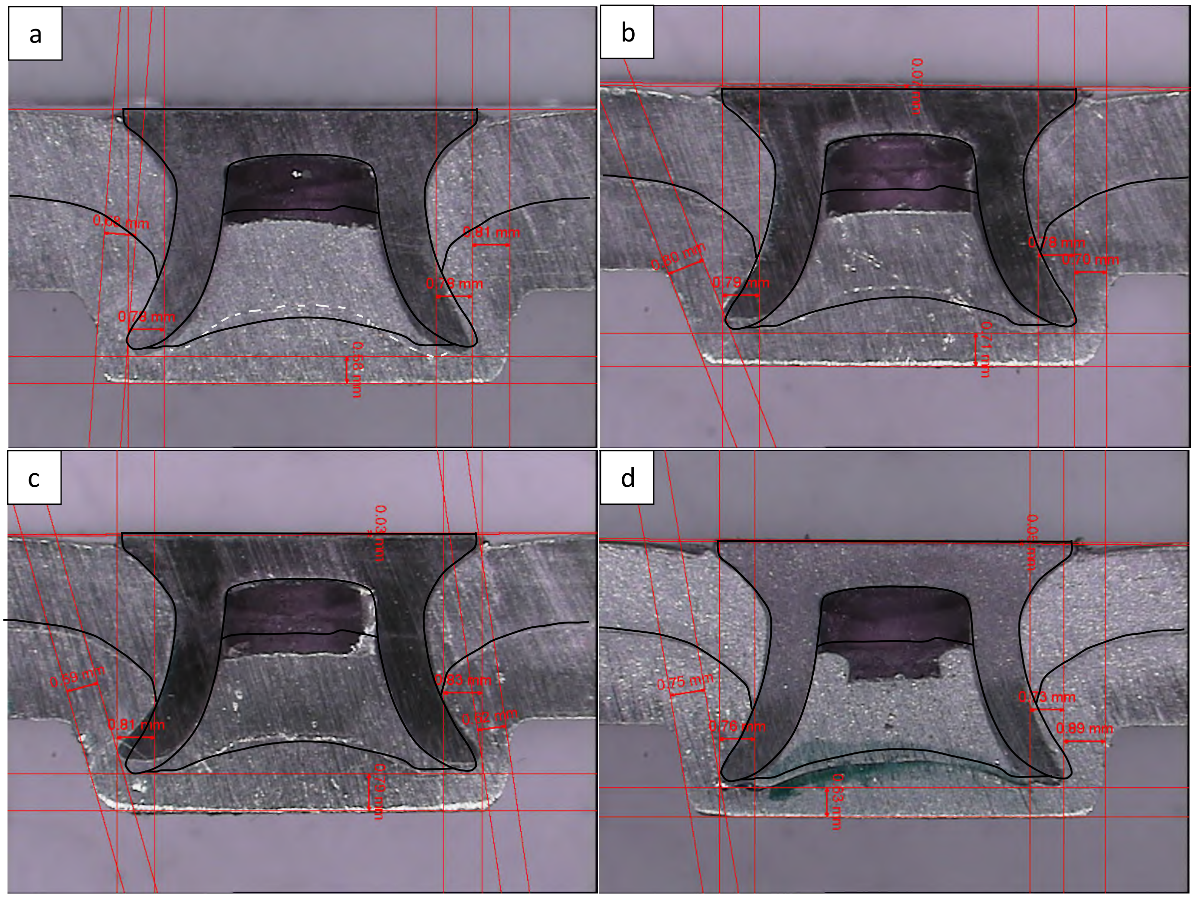

Figure 9 Cross section of (2+2)AA5754 SPR joints with the top sheet impressed by a central pin, a), impression only at the bottom surface, b) impression at the bottom surface with particles removed, c) impression at the bottom surface with particles remained, and d) impression only at the top surface.

Fig. 9 shows the cross sections of SPR joints after the top sheet local surface were modified in different ways. It can be seen that due to the work hardening introduced by the impression, the punched part of the top sheet had more difficulty to be pushed into the rivet cavity after impression on the top sheet, leaving larger portion of rivet cavity not filled. In the meantime, for the joints with the top sheet modified by the central pin and garnet particles, due to the increased friction between the punched portion of the top sheet and the bottom sheet interface and the mechanical interlocking from the impression hole, the deformation of the bottom sheet material became more difficult and less even. From Fig. 9 b and c, it can be seen that when the top sheet was impressed by central pin and garnet particles, the rivets flared more compared with those in the reference joints resulting in slightly larger interlocks. From Fig. 9a-c, it can be seen that after impression with the central pin, the punched portion of the top sheet pushed further into the rivet cavity (judged from the bottom surface profile of the punched portion of the top sheet) but leaving a larger volume not filled between the rivet head and the punched portion of the top sheet in the joints (judged from the top surface profile of the punched portion of the top sheet) compared with the reference joint. This meant that the punched portion of the top sheet was compressed into a smaller volume or had larger compress deformation in the joints with the top sheet impressed by the central pin.

Table 2 Summary of selected SPR joint features (All modifications were conducted on the bottom surface of the top sheet unless otherwise stated).

Joints	**Short names used in figures***	**Rivet head height, mm**	**Average interlocks, mm**	**T_{min} to the bottom, mm**	**T_{min} to the side, mm**	**T_{min} (overall), mm**
Reference	Reference	-0.08±0	0.78±0.03	0.67±0.02	0.7±0.07	0.67±0.02
Small ring impression only	S ring impression only	Similar to reference				
Small ring impression with particles removed	S ring impression P removed	0.01±0.02	0.8±0.07	0.75±0.06	0.73±0.08	0.7±0.02
Small ring impression with particles remained	S ring impression P remained	0.05±0.04	0.77±0.02	0.89±0.05	0.68±0.02	0.68±0.02
Medium ring impression only	M ring impression only	Similar to reference				
Medium ring impression with particles removed	M ring impression P removed	-0.03±0.04	0.78±0.02	0.72±0.01	0.8±0.03	0.72±0.01
Medium ring impression with particles remained	M ring impression P remained	-0.03±0.04	0.73±0.03	0.71±0.01	0.78±0.04	0.71±0.01
Small and medium rings impression with particles removed	S and M rings impression P removed	0.03±0.04	0.81±0.04	0.83±0.02	0.7±0.04	0.7±0.04
Small and medium rings impression with particles remained	S and M rings impression P remained	0.05±0.03	0.78±0.07	0.8±0.05	0.79±0.01	0.77±0.01
Large ring impression with particles removed	L ring impression P removed	Similar to reference				
Large ring impression with particles remained	L ring impression P remained	Similar to reference				
Central pin impression only at the top surface of the top sheet	C pin impression only at top surface	0.06±0.01	0.72±0.04	0.61±0.04	0.81±0.08	0.61±0.04

Central pin impression only	C pin impression only	-0.01±0.03	0.78±0.05	0.65±0.07	0.74±0.05	0.65±0.06
Central pin impression with particle removed	C pin impression P removed	0.02±0.04	0.79±0.08	0.67±0.05	0.75±0.05	0.67±0.05
Central pin impression with particle remained	C pin impression P remained	0.04±0.01	0.81±0.04	0.77±0.04	0.72±0.08	0.7±0.06

* ‘S’,’M’,’L’ mean small, medium and large respectively, ‘C’ means central, and ‘P’ means particles.

Table 2 summarises the joint features of some SPR joints. The joint features for the joints with ring impression only and with large ring impression were not summarised because they were similar to those for the reference joints. It can be seen that for all the joints modified by the ring impression the interlocks had no obvious change; however, the T_{min} was slightly increased and the rivet head height were slightly increased. As to the joints with the top sheet modified with the central pin, when an impression was applied on the top surface of the top sheet, the rivet head height of the joints increased and the interlock and the T_{min} of the joints decreased; when the top sheet was modified on the bottom surface of the top sheet, the rivet head height of the joints increased, the interlocks slightly increased, and the T_{min} of the joints did not have obvious change but with larger deviations. General speaking, when the bottom surface of the top sheet was modified with hard particles and with particles removed afterwards, the rivet head height increase would be larger than that for joints just having impression, and when the particles was remained in the joints after impression, the rivet head height would be even higher. Overall, the influence of local surface textures on the joint features was not significant.

3.2. SPR rivet inserting process

Fig. 10 shows the SPR rivet setting displacement-force curves for joints with and without local surface modification (except for the central pin modification on the top surface of the top sheet, all other modifications were on the bottom surface of the top sheet). To avoid the curves to be too messy, only some representative curves were included. It can be seen that the displacement-force curve for the joint with central pin impression on the bottom surface of the top sheet was almost the same as that for the reference joint. Although for most of the other joints with local surface modifications, the rivet setting forces were slightly higher between displacements of 2 and 7 mm, this difference was within the process deviation and overall the influence of local surface modification on the displacement-force curves was not significant.

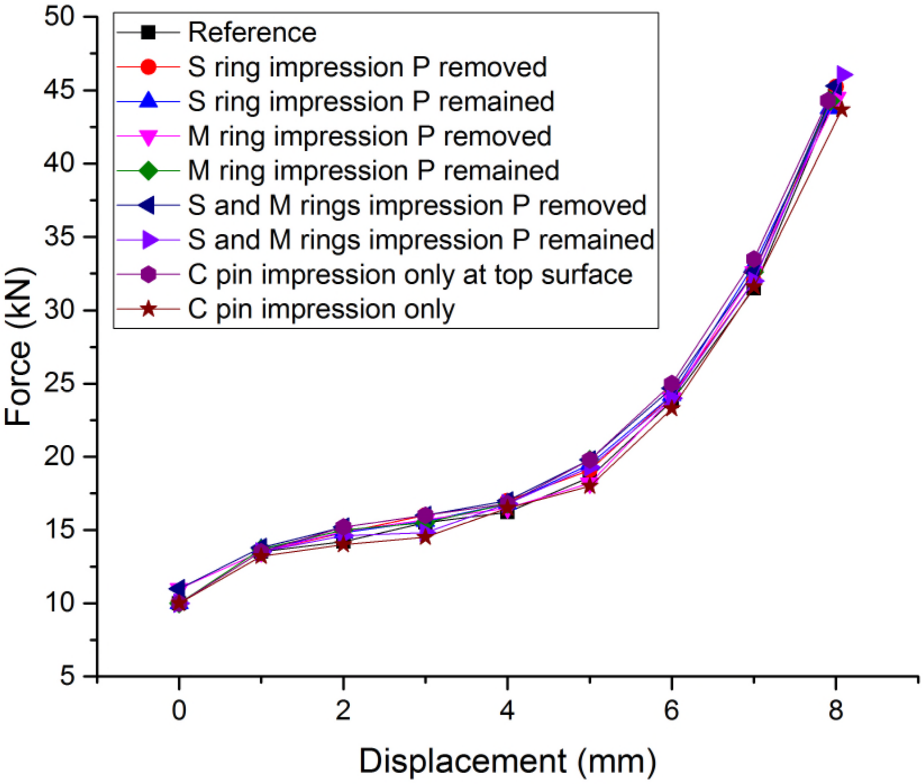

Figure 10 SPR riveting setting displacement-force curves.

3.3. SPR joint static lap shear strength

Fig. 11 presents the quasi-static lap shear strength of various specimens with or without local surface modification. It can be seen that central pin impression on the top surface of the top sheet did not change the lap shear strength of the joint; however, central pin impression on the bottom surface of the top sheet increased the joint strength. Local impression only (without hard particles) with different size of rings close to the rivet piercing location did not increase the joint strength; however, when hard particles, like garnet, were used to increase the local surface roughness at the impression locations, joint strength was greatly increased. The largest joint strength increase for a single ring impression occurred when the small ring was used to impress the local surface and the particles were left on the surface when the joints were made. Another phenomenon can be seen was that for the joints with the garnet particles were left at the surface after impression the lap shear joint strength was much higher than that for the joints with the particles removed after impression. When the combined impression from the small and medium rings were applied, the joint lap shear strength increased slightly further compared with that from the joints with the top sheet impressed by the small ring only.

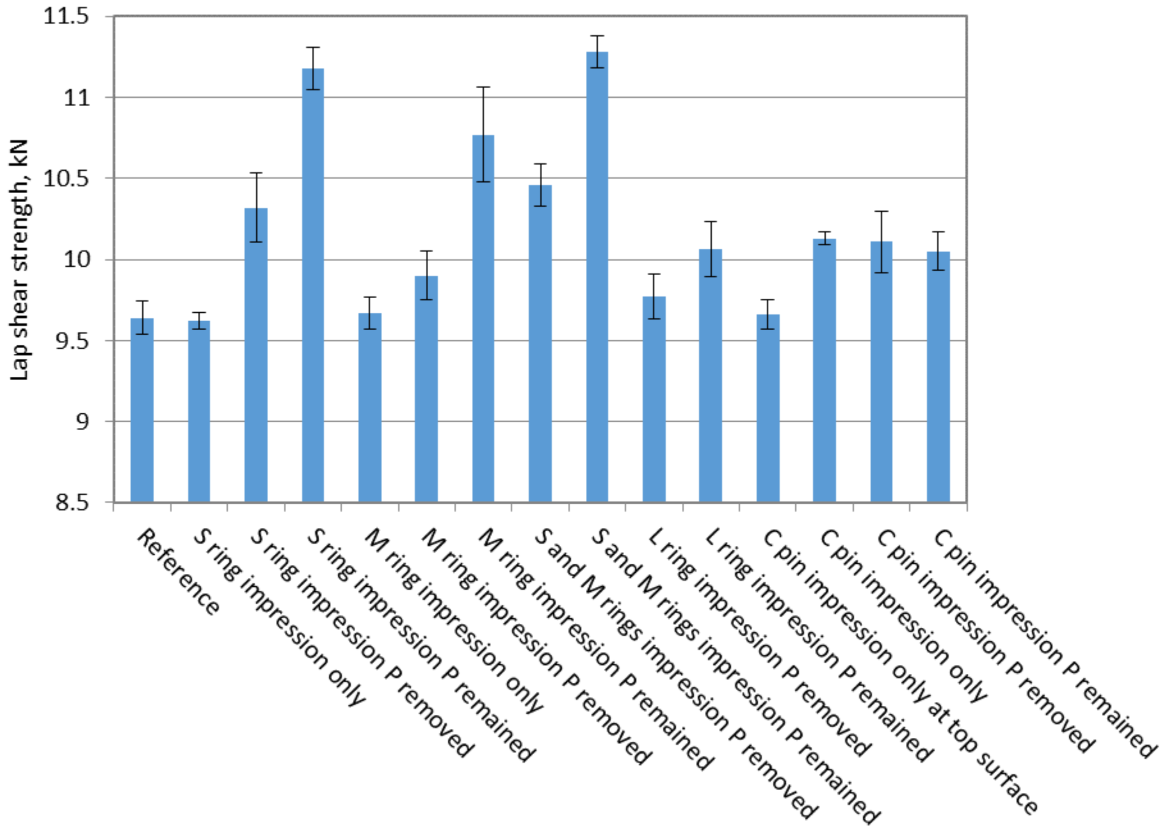

Figure 11 Quasi-static lap shear strength of specimens.

4. Discussion

4.1 Influence of local surface texture on rivet inserting process

From the results in Sections 3.1 and 3.2, it can be seen that different local surface texture through impression could have some influence on the joint quality and rivet inserting displacement-force curves, but this influence was not significant. This can be explained through the deformation and plastic flow of the top and bottom sheets during the riveting process.

Hou et al. [17] studied the typical four-stage displacement-force curves of SPR rivet inserting process, and later on Bouchard et al. [18] also used Forge2005® finite element code to model SPR process for rivetability prediction and compared it with experimental results. Both of the studies showed that there was a gap formed between the top sheet and the bottom sheet just after the rivet penetrated the top sheet and started to pierce the bottom sheet when a die with a pip at the bottom was used, and this gap was closed up during later rivet setting process. Haque et al. [19] studied the displacement-force curves of self-piercing riveting carbon steels with a flat bottom die. Gaps between the top and the bottom sheet during rivet inserting process were also reported due to the difference of material flow. For the material stack and rivet/die combination we studied, a flat bottom die was used and similarly gaps formed between the top and bottom sheets during the rivet inserting process were found. Fig. 12 shows the force-displacement curve of the SPR process for the combination studied with joint cross sections at different rivet inserting stages. It can be seen that from the beginning of rivet setting, there was a gap between the top and the bottom sheet due to no intimate contact. When the rivet started to pierce the bottom sheet, the gap between the top and the bottom sheet underneath the rivet cavity was closed up, but outside the rivet inserting location, and this gap was still existing. The gap at the location immediately next to the rivet inserting location became larger, due to the higher degree of bending of the bottom sheet than the top sheet. This gap was not closed up until the very late stage of the rivet setting process when the rivet head started to contact and apply force to the top sheet. The largest gap was existing between the clamping locations and the rivet skirt/legs during these stages.

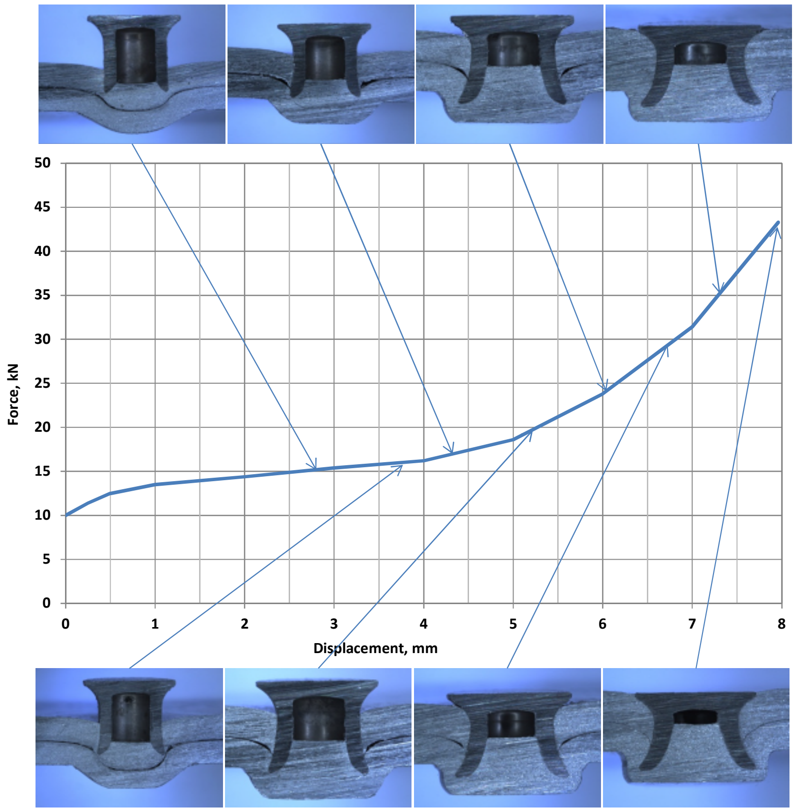

Figure 12. The force-displacement curve of the SPR process for the material stack and rivet/die combination with joint cross sections at different rivet inserting stages.

Although during a SPR riveting process, the friction between the top and bottom sheet has some influence on the inserting force, rivet deformation and joint quality, due to the existing of gaps and no intimate contact between the top and bottom sheets, especially at the locations with large plastic flow (between the clamping locations and the rivet skirt/legs), it is believed that the friction between the top and the bottom sheets outside the rivet penetration location during a riveting process is not large and have no significant influence on the rivet inserting process and joint quality. As a result, when the bottom surface of the top sheet was locally modified with different texture outside the rivet penetration location, it had no significant influence on the joint quality and rivet inserting displacement-force curves. As to friction during a rivet inserting process, it is believed that the friction between the rivet and the substrate materials and the friction between the top and the bottom sheets at other locations, such as between the punched top material and the bottom material, may have more significant influence on the inserting process. Other factors that influence the rivet inserting displacement-force curves include the mechanical properties of rivet and sheet materials, the dimensions and geometries of the die and rivet, and the material stack.

4.2 Influence of local surface texture on static lap shear strength

To understand the factors that can influence the static lap shear strength of a SPR joint, it is very important to understand the mechanical states of the SPR joint during a static lap shear test. Fig. 13 shows some of the critical locations and their mechanical states during a static lap shear test. It can be seen that there are four critical friction locations: 1 to 4, and two critical compression force locations: 5 and 6, due to the pulling and secondary bending from the top and bottom sheets. Location 1 is at the interface between the rivet and the top sheet on the tension side: location for main friction when the rivet head is pulled out of the top sheet; location 2 is at the interface between the rivet and the bottom sheet on the tension side: location for main friction when the rivet skirt is pulled out of the bottom sheet; location 3 is at the interface between the top and bottom sheets around the tip of the punched hole in the top sheet on the tension side: location for main friction between the top and bottom sheets; location 4 is at the interface between the rivet and the bottom sheet underneath the rivet skirt: friction location when the rivet is forced to rotate; location 5 is at the interface between the rivet and the top sheet on the compression side: location for main compression force between the rivet and the top sheet; location 6 is at the interface between the rivet and the bottom sheet on the compression side: location for main compression force between the rivet and the bottom sheet. The compression at locations 5 and 6 was the result of the applied shear forces. There were compressions and relative movements at the four critical friction locations, and the compressions at these locations could be from difference sources, such as the residual stress from rivet setting process (residual stress), and the bending of sheet material (sheet bending) and the rotating of the rivet (rivet rotating) during the lap shear test. The compression at locations 1 and 2 was from residual stress which has been reported before [20-24] and rivet rotating, and the compression at location 3 was from residual stress and sheet bending. The friction forces will influence the lap shear strength [5], and the compression forces at locations 5 and 6 will cause the rivet to rotate and the sheet material to be deformed during a static lap shear test. Fig. 13 is only a 2D schematic diagram showing the cross section along the central line, and for 3D concept the locations has to be treated as curved surfaces around that locations. In this study, for first 11 stacks listed in Table 2, because only the bottom surface of the top sheet was modified, the main factor that would influence the lap shear strength would be related to location 3.

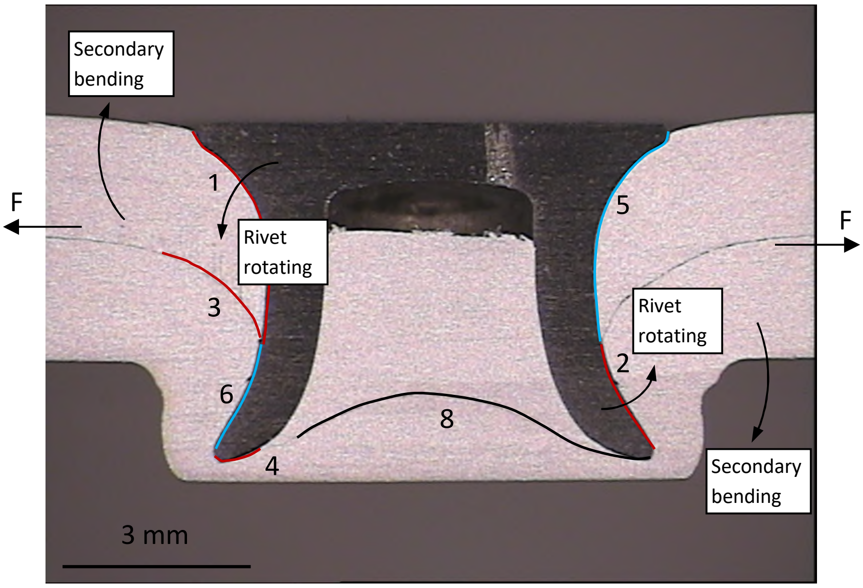

Figure 13 Critical locations and their mechanical states during a static lap shear test.

Results from Li et al. [6] pointed out that the friction force between the tip of the punched hole in the top sheet and the edge of the partially pierced hole in the bottom sheet was very important for static lap shear strength. Their results showed that fretting during fatigue increased friction force between the tip of the punched hole in the top sheet and the edge of the partially pierced hole in the bottom sheet, and as a result the remaining static lap shear strength of the specimens was increased. One purpose of this research is to prove the importance of this local friction and confirm the critical locations.

Fig. 14 shows the fracture interfaces of some specimens after lap shear tests. The friction marks on the fracture interfaces showed that during lap shear tests the main friction between the top and the bottom sheets was at location 3, at the interface between the top and bottom sheets interface around the tip of the punched hole in the top sheet, as shown in Fig. 13.

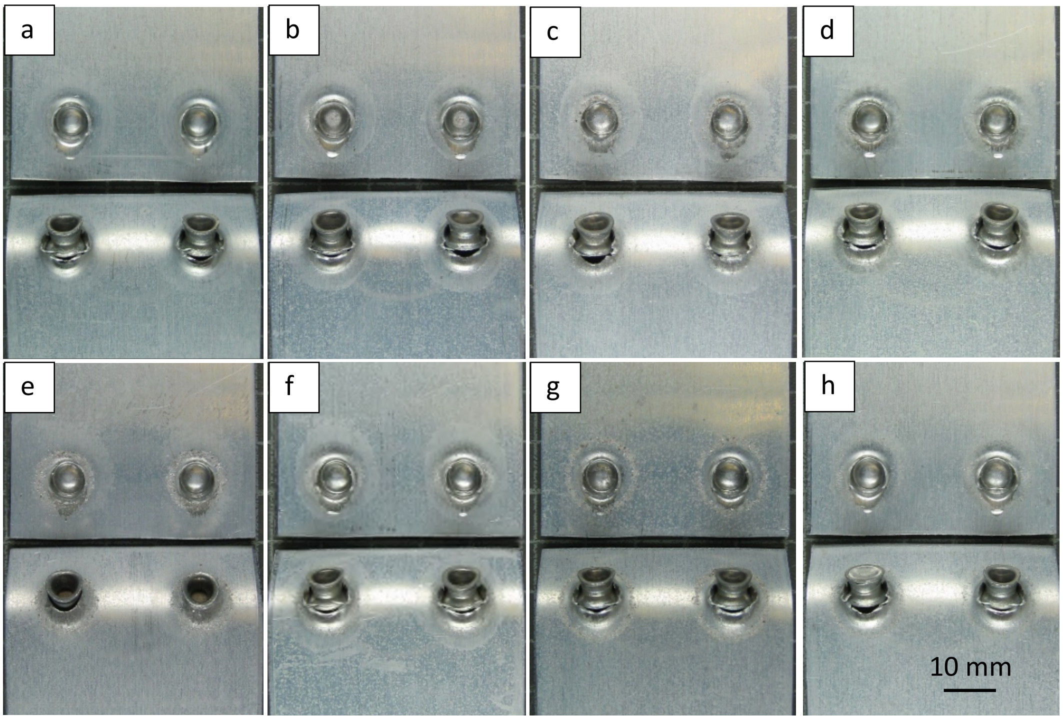

Figure 14 Fracture interfaces of specimens with local impression on the bottom surface of the top sheet after lap shear tests, a) reference, b) central pin impression with particles remained, c) small ring impression with particle remained, d) small ring impression with particles removed, e) medium ring impression with particle remained, f) medium ring impression with particles removed, g) large ring impression with particle remained, and h) large ring impression with particles removed.

4.2.1 Locations outside the piercing ring

The lap shear results in Fig. 11 show that local surface texture (modified by the impression rings) close to and outside of the rivet piercing circle could increase the static lap shear strength of the SPR joints. There are two effects on the substrate when an impression with hard particles is conducted on the surface: one is work hardening and the other is the increase of surface roughness and subsequently local friction.

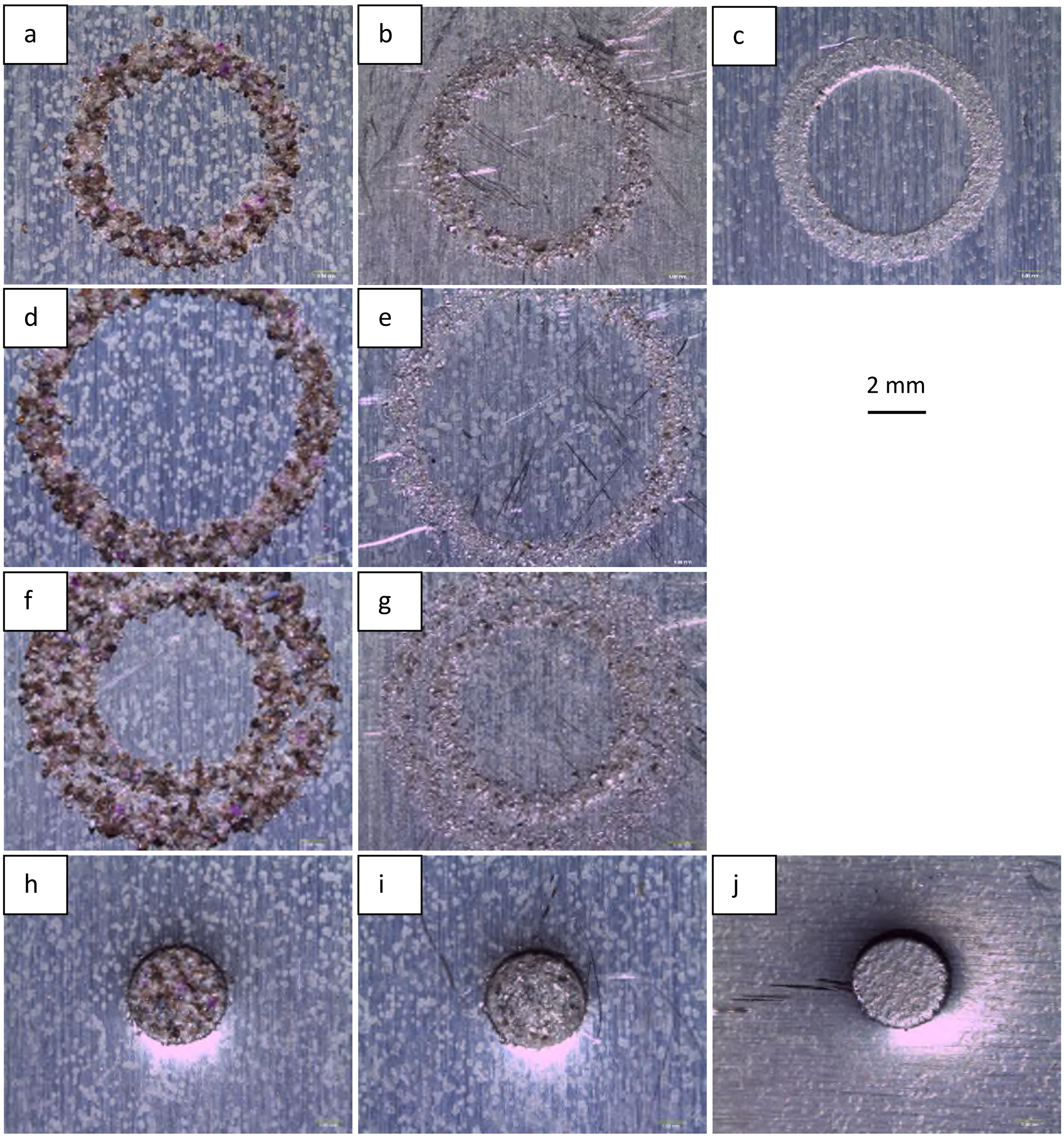

Figure 15 Local textures and deformation of the coupons for lap shear specimens after surface modifications, a) small ring impression with particles remained, b) small ring impression with particles removed, c) small ring impression only, d) medium ring impression with particles remained, e) medium ring impression with particles removed, f) small and medium rings impression with particles remained, g) small and medium rings impression with particles removed, h) central pin impression with particles remained, i) central pin impression with particles removed and j) central pin impression only.

Fig. 15 shows local textures and deformation of the coupons for lap shear specimens after impressions. It can be seen that for coupons impressed with particles and with particles removed afterwards, the local surface became much rougher (Fig. 15b, e, g and i); for coupons impressed with particles and with particles remained, some particles were imbedded in the substrate (Fig. 15a, d, f and h); for coupons with ring impression only the surface was still very smooth with a shallow impression mark (mainly from deformed solid wax, Fig. 15c). For joints with local impression only, it was assumed that only work hardening effect existed since the impression did not increase the local roughness.

Because the impression marks for all the impression with different size of rings were very shallow, it is believed that the work hardening to the local bulk material was very small, and as a result the influence of work hardening on joint strength by ring impression would be very little. This was confirmed by the insignificant joint strength increase of the joints with local impression only. For joints with local ring and hard particle impression, it can be assumed that the work hardening to the local bulk material was similar to that for the joints with local impression only and was not significant. This means that the main influence of local ring impression on the joint lap shear strength is from the increase of local friction. It is believed that the local friction would increase with the increase of roughness. Also, when hard particles were remained in the joints, during rivet inserting and following lap shear test, the hard particles would penetrate into the mating surface (the top surface of the bottom sheet that was not modified) as well, which will further increase the friction force at the local interface. The influence of local friction on joint lap shear strength was confirmed by the results presented in Fig. 11. It showed that for all the joints with impression with different size of rings and hard particles, the lap shear strength increased, and the joints with particles remained had further higher joint strength for the same location of impression modification.

It may be argued that the lap shear strength increase could be caused by different joint features, especially joint interlocks, but the results in Table 3 showed that the joint features for all the joints did not have significant difference. On the contrary, when the same impression ring was used, the interlock distances for the joints with particles remained were slightly lower than those for the joints with particles removed, although the lap shear strength for the former was higher.

Friction at the top and the bottom sheet interface is important, but this does not mean that the entire mating surface between the top and the bottom sheet is important, because there are only certain areas that are friction critical as analysed in Fig. 13. The friction marks on the fracture interfaces in

Fig. 14 showed that during lap shear tests the main friction between the top and the bottom sheets was around the tip of the punched hole in the top sheet on the tension side. Fig. 14 showed that the friction severity for specimens impressed with different sizes of rings is in the following orders: 1. Small ring>medium ring>large ring and 2. Impression with particles remained>impression with particles removed>reference or central pin impression. This is consistent with the increase of the joint lap shear strength. It worth pointing out that when the sheet surface was modified with local rings and with particles remained, the remained particles might spread into the area around during riveting and subsequent lap shear tests. This may be the reason that for the joints with medium ring impression and with particles remained, the friction at the tip of the punched hole of the top sheet (the area normally covered by the small ring impression) (Fig.14e) was much severer than the friction for the joints with medium ring impression and with particles removed (Fig.14f). Fig. 16 shows the optical images of the friction marks at the bottom surface of the top sheet around the punched hole of the three selected specimens after lap shear tests. Fig. 16a shows that when the sheet material had the original surface, after the lap shear test, only some shallow friction marks could be seen at the tip of the punched hole; Fig. 16b shows that when the sheet material was locally modified by the small ring and with particles removed, some deep friction marks left at the tip of the punched hole; Fig. 16c shows that when the sheet material was locally modified by the small ring and with particles remained, the surface at the tip of the punched hole was worn down and some friction debris left on the surface. The friction marks in Fig. 16a were about 1.5 mm long, the friction marks in Fig. 16b were about 2.2-2.5 mm long and the friction marks in Fig. 16c were about 3 mm (not completely covered by the image). This result together with fracture interfaces in Fig. 14 can confirm that the friction marks were mainly within the small and medium ring impression areas (between 0 and 3 mm to the edge of the punched hole). Fig. 16 also showed that the most severe wear on the top sheet was at an area about 0-1.5 mm away from the edge of the punched hole.

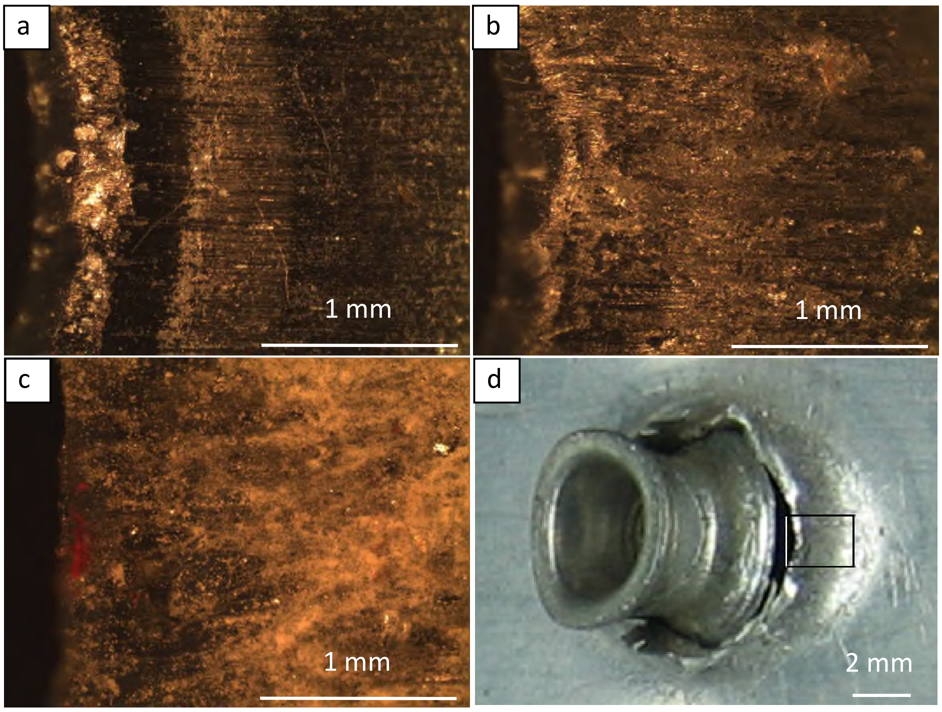

Figure 16 Multi-focus optical microscope images of the friction marks at the bottom surface of the top sheet around the pierced hole of three selected specimens after lap shear tests, a) reference, b) small ring impression with particles removed, c) small ring impression with particles remained and d) location of the optical images indicated by the rectangle.

The results in Figs. 11 and 14 can also confirm the critical locations of the local friction. Fig. 11 showed that with a single ring impression the largest lap shear strength increase was generated by the impression with the small ring and with hard particles remained. With the increase of ring size, it can be seen that the lap shear strength increase compared to the reference specimens was getting smaller. When the impressions from the small ring and the medium ring were both applied, the lap shear strength of the joints increased slightly further, compared with the joints with impression from the small ring only. It can be seen that the critical location for friction influence was at the small ring impression location, which was a small area next to the rivet piercing site at the top and the bottom sheet interface. After the joint was formed, the location would be at the top and bottom sheet interface around the tip of the punched hole in the top sheet. When the location moved further away from the tip or rivet skirt/legs, the local friction would have less influence on joint lap shear strength.

4.2.2 Locations inside the piercing ring

From Fig. 15, it can be seen that the deformation caused by the ring impression was very small, and on the contrary, the deformation caused by the central pin impression was large, leaving an impression hole and a dent around. These different deformations were caused by the different size of impression heads. For the central pin, the impression area is 8 mm^2, and for the small ring, the impression area is 32 mm^2. It is believed that the work hardening caused by the central pin impression was substantial and the work hardening caused by the ring impressions was small.

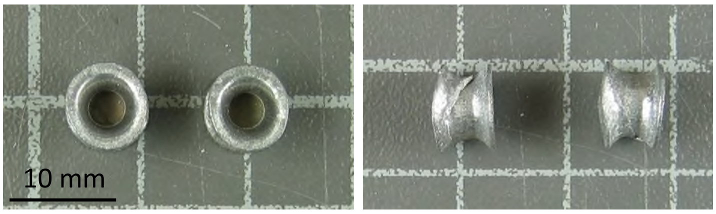

Figure 17 Deformation of SPR rivets during lap shear tests.

The lap shear results in Fig. 11 show that local surface texture (modified by the central pin) in the centre of the rivet piercing circle could also increase the static lap shear strength of SPR joints. The results showed that when the pin impression was conducted on the top surface of the top sheet, the static lap shear strength had no obvious increase, but when the impression was conducted on the bottom surface of the top sheet, the lap shear strength increase was about 0.5 kN. It can be seen that increase the local surface roughness by impression with hard particles did not increase the lap shear strength further. Obviously, if there was friction at this central location during lap shear tests, the friction force would be increased by the local roughened surface. However, from the fracture interface of failed lap shear specimens and the mechanical states described in Fig. 13, it was found that during a lap shear test, due to the secondary bending of the sheet material and the rotating of the rivet, a gap would be generated between the punched portion of the top sheet and the bottom sheet interface (as shown in location 8 in Fig. 13). Due to the existing of this gap, no substantial friction would occur at this location, and as a result increase of the local surface roughness at the pin impression location did not increase the lap shear strength further. It is believed that the lap shear strength increase for joints with the bottom surface of the top sheet impressed by the pin was caused by local work hardening.

From Fig. 9a-c, it can be seen that compared with the reference joint, in the joints with the bottom surface of the top sheet impressed by the pin, the punched material from the top sheet had larger total compression deformation (including the deformation caused by pin impression), and as a result, its remained volume was smaller and a larger cavity between the rivet head and the punched material was left. Larger deformation would mean larger work hardening and higher strength for the punched material. Although the punched material does not play a big role during joint lap shear deformation, it gives support to the rivet skirt and the deformation of rivet skirt is important to joint strength. Although rivets are much stronger than the aluminium alloy substrates, evidence showed that they did deform during lap shear tests, as shown in Fig. 17 (rivet skirt squeezed in one direction). It is believed that the stronger support from the punched material made the rivet skirt less easy to be squeezed/bent back, and consequently increased the joint strength. However, when the impression was conducted on the top surface of the top sheet, the strength of the upper part of the punched material from the top sheet increased, which would make the punched top material more difficult to be pushed into the rivet cavity, leaving a larger gap between the rivet head and the top of the punched material, as shown in Fig. 9d. Since the support of rivet skirt from the lower part was more effective than that from the upper part against compression, no obvious lap shear strength increase could be seen in this case.

5. Conclusions

To study the influence of local frictions on rivet inserting process, joint features and static lap shear strength, the surface of the top sheet has been locally modified around the rivet piercing location with different impression tools and garnet particles. The following conclusions can be drawn:

1) The studied local surface textures on the aluminium sheet did not have significant influence on the rivet inserting process based on displacement-force curve analysis.

2) The local surface textures studied could slightly change the joint features, especially the rivet head height, but overall this influence was also not significant.

3) The lap shear tests showed that ring impressions with garnet particles and central pin impressions on the bottom surface of the top sheet increased the static lap shear strength of the SPR joints. The strength improvement from local ring impressions with particles was by increasing local friction and the strength improvement from central pin impressions was by local work-hardening.

4) It was confirmed that the critical location for local friction influence on the lap shear strength was around the rivet leg piercing location or in other words around the tip of the punched hole in the top sheet after rivet inserting.

Acknowledgement

The authors would like to thanks Innovate UK for the support of this research through HVM Catapult. The authors would also like to thanks Henrob Ltd for providing the rivets for this research.

References

[1] Li D, Chrysanthou A, Patel I, Williams G, Self-piercing riveting-a review, Int J Adv Manuf Tech, 2017, doi:10.1007/s00170-017-0156-x.
[2] Chapter 33 Bolted connections-I, www.steel-insdag.org/TeachingMaterial/chapter33.pdf; 2000 [accessed 20.06.17].
[3] Bolted Joint Design - Fastenal, https://www.fastenal.com/content/feds/pdf/Article%20-%20Bolted%20Joint%20Design.pdf; 2009 [accessed 20.06.17].
[4] Han L, Chrysanthou A, Evaluation of quality and behaviour of self-piercing riveted aluminium to high strength low alloy sheets with different surface coatings, Mater Design, 2008; 29: 458-68.
[5] Han L, Chrysanthou A, O'Sullivan JM, Fretting behaviour of self-piercing riveted aluminium alloy joints under different interfacial conditions, Mater Design, 2006; 27: 200-8.
[6] Li D, Han L, Thornton M, Shergold M, Williams G, The influence of fatigue on the stiffness and remaining static strength of self-piercing riveted aluminium joints, Mater Design, 2014; 54: 301-14.
[7] Han L, Young KW, Hewitt R, Alkahari MR, Chrysanthou A, Effect of sheet material coatings on quality and strength of self-piercing riveted joints, in: SAE World Congress, Paper No. 2006-01-0775, 2006.
[8] Xu Y, A close look at self-piercing riveting-Computer simulation is a noteworthy alternative to physical testing of joints, in: The Fabricator, 2006.
[9] Khezri R, Sjöström E, Melander A, Self-piercing riveting of high strength steel, in: Swedish Institute for Metal Research, Report No. IM-2000-554, 2000.
[10] Abe Y, Kato T, Mori K, Self-piercing riveting of high tensile strength steel and aluminium alloy sheets using conventional rivet and die, J Mater Process Tech, 2009; 209: 3914-22.
[11] Krishnappa US, Numerical Investigation of self-piercing riveted dual layer joint, in: Department of Mechanical Engineering, Master thesis, Wichita State University, India, 2004.

[12] Atzeni E, Ippolito R, Settineri L, Experimental and numerical appraisal of self-piercing riveting, CIRP Ann Manuf Technol, 2009; 58: 17-20.
[13] Carandente M, Dashwood RJ, Masters IG, Han L, Improvements in numerical simulation of the SPR process using a thermo-mechanical finite element analysis, J Mater Process Tech, 2016; 236: 148-61.
[14] Han SL, Tang XD, Gao Y, Zeng QL, Effects of friction factors on flat bottom self-pierce riveting joints of AZ31 magnesium alloy, Mater Res Innov, 2015; 19: S10-235-38.
[15] Li D, Han L, Thornton M, Shergold M, Influence of edge distance on quality and static behaviour of self-piercing riveted aluminium joints, Mater Design, 2012; 34: 22-31.
[16] Li D, Han L, Thornton M, Shergold M, Influence of rivet to sheet edge distance on fatigue strength of self-piercing riveted aluminium joints, Mat Sci Eng A-Struct, 2012; 558: 242-252.
[17] Hou W, Mangialardi E, Hu SJ, Wang PC, Menassa R, Characterization for Quality Monitoring of a Self-Piercing Riveting, in: Sheet Metal Welding conference XI, Sterling Heights, Michigan, 2004, Paper No. 8-3.
[18] Bouchard PO, Laurent T, Tollier L, Numerical modeling of self-pierce riveting-From riveting process modeling down to structural analysis, J Mater Process Tech, 2008; 202: 290-300.
[19] Haque R, Beynon JH, Durandet Y, Characterisation of force-displacement curve in self-pierce riveting, Sci Technol Weld Joi, 2012; 17: 476-88.
[20] Huang L, Moraes JFC, Sediako DG, Jordon JB, Guo H, Su X, Finite-Element and Residual Stress Analysis of Self-Pierce Riveting in Dissimilar Metal Sheets, J Manuf Sci E T ASME, 2017; 139: 021007-1 - 11.
[21] Haque R, Wong YC, Paradowska A, Blacket S, Durandet Y, SPR Characteristics Curve and Distribution of Residual Stress in Self-Piercing Riveted Joints of Steel Sheets, Adv Mater Sci Eng, 2017, doi:10.1155/2017/5824171.
[22] Han L, Chrysanthou A, Young KW, Mechanical behaviour of self-piercing riveted multi-layer joints under different specimen configurations, Mater Design, 2007; 28: 2024-33.
[23] Haque R, Wong YC, Paradowska A, Durandet Y, Residual stress profiles in riveted joints of steel sheets, Sci Technol Weld Joi, 2015; 20: 199-207.
[24] Huang L, Lasecki JV, Guo H, Su X, Finite element modeling of dissimilar metal self-piercing riveting process, SAE Int J Mater Manuf, 2014; 7: 698-705.